Forest height estimation methods using polarimetric SAR interferometry

LUO Huanmin[1], CHEN Erxue[2], CHENG Jian[3], LI Xiaowen[1, 4]

1. *Institute of Geo-spatial Information Science and Technology*, *University of Electronic Science and Technology of China*, *Sichuan Chengdu* 610054, *China*;
2. *Institute of Forest Resources Information Technique of Chinese Academy of Forestry*, *Beijing* 100091, *China*;
3. *School of Electronic Engineering*, *University of Electronic Science and Technology of China*, *Sichuan Chengdu* 610054, *China*;
4. *Research Center for Remote Sensing and GIS*, *School of Geography*, *Beijing Normal University*, *Beijing* 100875, *China*

Abstract: Forest height extraction with polarimetric SAR interferometry (POLInSAR) is a hot research field of imaging SAR remote sensing. Several available forest height inversion methods using POLInSAR data were validated and compared with repeat pass E-SAR datasets and the corresponding ground measured forest stand height through the analysis of the Random Volume over Ground (RVoG) scattering model. After analyzing the experiment results in the view of physical mechanisms, we developed an integrated inversion method combining interferometric coherence optimization and compensation of non-volumetric scattering decorrelation. Validation result shows that the general performance of the developed forest height inversion method is superior to the others.

Key words: POLInSAR, polarimetric interferometric coherence optimization, RVoG, forest height, non- volumetric scattering decorrelation

CLC number: TP722.6/S7 **Document code:** A

Citation format: Luo H M, Chen E X, Cheng J and Li X W. 2010. Forest height estimation methods using polarimetric SAR interferometry. *Journal of Remote Sensing*. **14**(4): 806—821

1 INTRODUCTION

The forest height is an important forest resource information parameter and usually used in biomass estimation model. Forest height extraction with polarimetric SAR interferometry (POLInSAR) is a hot research field of imaging SAR remote sensing. SAR interferometry is a well-established SAR technique to estimate the vertical location of the effective scattering center in each resolution cell through the phase difference in images acquired from spatially separated antennas. Scattering polarimetry is sensitive to the shape, orientation and dielectric properties of scatterers. POLInSAR based on the coherent combination of radar interferometry and polarimetry allows us to overcome the severe limitations of both techniques when taken alone and is becoming an important technique for forest parameters extraction (Wu *et al*., 2007). Cloude *et al.* (2003) have proposed the three-stages inversion algorithm which is based on a coherent mixture model of a random volume over ground describing the relation of forest height and polarimetric interferometric coherence. A two–component polarimetric interferometric model is presented for improvement of vegetation parameter retrieval using the Nelder–Mead simplex optimal method. It combines scattering model based polarimetric decomposition technique and RVoG based POLInSAR forest parameters inversion model (Neumman *et al.*, 2009). Hajnsek *et al.* (2009) discussed the effect of some factors, such as temporal decorrelation and topography etc., to forest height inversion accuracy using P-, L- and X-band airborne POLInSAR data of Indonesia’s tropical forests.

The error sources of POLInSAR forest height inversion has been qualitatively analyzed using SIR-C/X SAR L-band repeat pass POLInSAR data and the corresponding optical image acquired in Hetian of Xinjiang (Chen *et al*., 2007). Six forest tree height inversion methods of POLInSAR were validated using repeat pass E-SAR datasets and the corresponding ground measured forest stand height (Chen *et al*., 2008). Utilizing the differences among the powers of backward scattering signal and scattering centers with different scattering mechanism in the same resolving unit, some scholars proposed TLS-ESPRIT algorithm to extract dominant scattering center phases for forest tree height inversion. The method can improve computational efficiency, but the capability for improving inversion accuracy is limited (Yang *et al*., 2007; Zhou *et al.*, 2008). In order to

Received: 2009-09-11; **Accepted**: 2010-02-01

Foundation: National Nature Sciences Foundation (No. 2007CB714404).

First author biography: LUO Huanmin (1972—), male. He received master degree from the School of Automation Engineering, University of Electronic Science and Technology of China (UESTC). He is now studying for Ph.D. Degree in Institute of the Geo-spatial Information Science and Technology, UESTC. His research interests are mainly the polarimetric and interferometric SAR remote sensing for forest applications.E-mail:Lhm123345@qq.com

improve the accuracy of forest tree height estimation, Li *et al*. (2005)and Chen *et al*. (2008) carried out relevant research work trying to increase the utilization of baseline or frequency information in observation space.

After analyzing the experiment results of several available forest height inversion methods in the view of physical mechanisms, a RVoG model based inversion model combining coherent amplitude with phase information is developed in this paper, where the Phase Diversity (PD) interferometric coherence optimization method (Tabb *et al*., 2002) is used to obtain the surface and volume scattering phase. In order to investigate better inversion methods, the performance of the proposed method is compared with the other available methods using repeat pass E-SAR L band POLInSAR data and the corresponding ground measured forest stand height.

2 TEST SITES AND DATA SETS

Repeat pass POLInSAR data of the test site Traunstein in Germany acquired by the E-SAR L-band SAR sensor of DLR in 2003 is used for the study. The flight altitude is about 3000m above ground; the horizontal spatial baseline is 5m and the temporal baseline is 20min. The incidence angle increases from 25° in near range to 60° in far range. The data were processed for 1.5m range resolution and 3.0m resolution in azimuth.

The study area is mainly covered by agricultural fields, pasture, forests and some urban area in the western part of it, where the city of Traunstein is located. The topography is flat with elevation varying from 600 to 650m. The dominant tree species of this site is composed of spruce, beech and fir. The mean dominant height of forest stand (h_v means the mean height of the 100 highest trees per hectare) of 20 validation stands is estimated by means of detailed forest inventory. These validation stands are characterized by mixed mountainous forests with individual tree height up to 40m and a mean biomass level up to 450 t/hm^2.

Fig.1 shows the Pauli-basis E-SAR L-band image for the Traunstein scene in RGB color combination. It can be seen that the forest regions appear green to white color indicating that volume scattering possess a comparably strong HV/VH response. There are also some double bounce scattering phenomena around the forest stand borders by the trunk-ground interaction.

In Fig.2, the average coherence amplitude and phase in HH, HV, VV and HH-VV polarization channel is plotted respectively against the ground measured upper canopy height of the 20 validation stands (Fig.1). As shown in Fig.2 (b), the difference of the mean coherence phase among the polarization channels is small. It can be seen from Fig.2 (a) that the coherence amplitude of each polarization channel is obviously more sensitive to forest height, but the difference between polarization channels is small. From these, we can see that a variety of scattering mechanisms and factors contribute to the polarization coherence. So, forest height inversion methods only based on the separation of scattering mechanisms have bigger forest height estimation error. In order to improve the inversion accuracy, some models and methods were proposed in recent years. In the paper, the performance of these forest height inversion algorithms are quantitatively discussed and evaluated using the POLInSAR dataset and some ground truth data in forest stand scale. The flow chart of this study is shown in Fig.3.

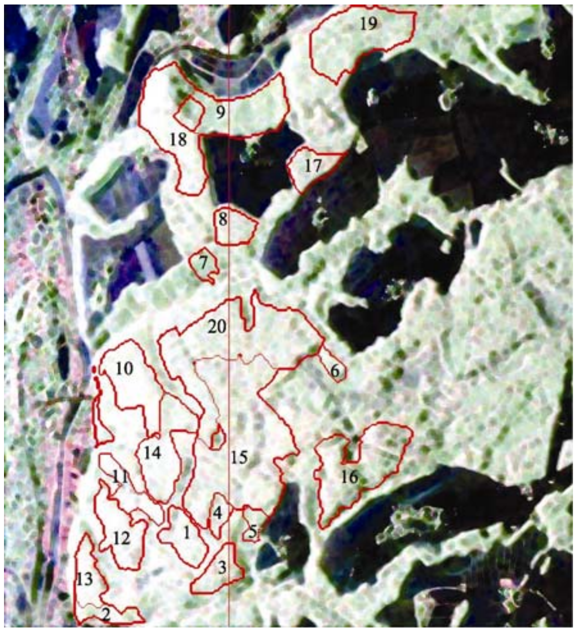

Fig. 1 PAULI decomposition RGB image of the polarimetric SAR data of the test site

3 INVERSION METHOD WITHOUT ASSUMING STRUCTURE FUNCTION

This method was first proposed by Cloude and Papathanassiou (1998) as DEM differencing approach, but it is better to name it as DSM differencing approach. Without assuming a forest vertical structure reflectivity function, the method simply define forest height as a phase difference between interferogram of the polarization channel dominated by "pure" volume scattering from the forest canopy top and that of the polarization channel dominated by "pure" surface scattering from the ground surface. Forest height is obtained through the phase difference divided by the effective wave number as Eq. (1).

$$h_{\mathrm{v}} = \frac{\arg(\gamma_{\boldsymbol{w}_{\mathrm{v}}}) - \arg(\gamma_{\boldsymbol{w}_{\mathrm{s}}})}{k_{\mathrm{z}}},$$

where

$$k_{\mathrm{z}} = \frac{4\pi\Delta\theta}{\lambda\sin\theta} \tag{1}$$

where k_z is the effective wave number, θ is the angle of incidence and $\Delta\theta$ is the apparent angular separation of the baseline from the scattering point, $\gamma_{\boldsymbol{w}_{\mathrm{v}}}$ is complex coherence corresponding "pure" volume scattering mechanism for the top forest canopy, $\gamma_{\boldsymbol{w}_{\mathrm{v}}}$ is complex coherence corresponding to "pure" surface scattering mechanism for the under-canopy ground surface. HV polarization is selected to obtain $\gamma_{\boldsymbol{w}_{\mathrm{v}}}$, while cohe-

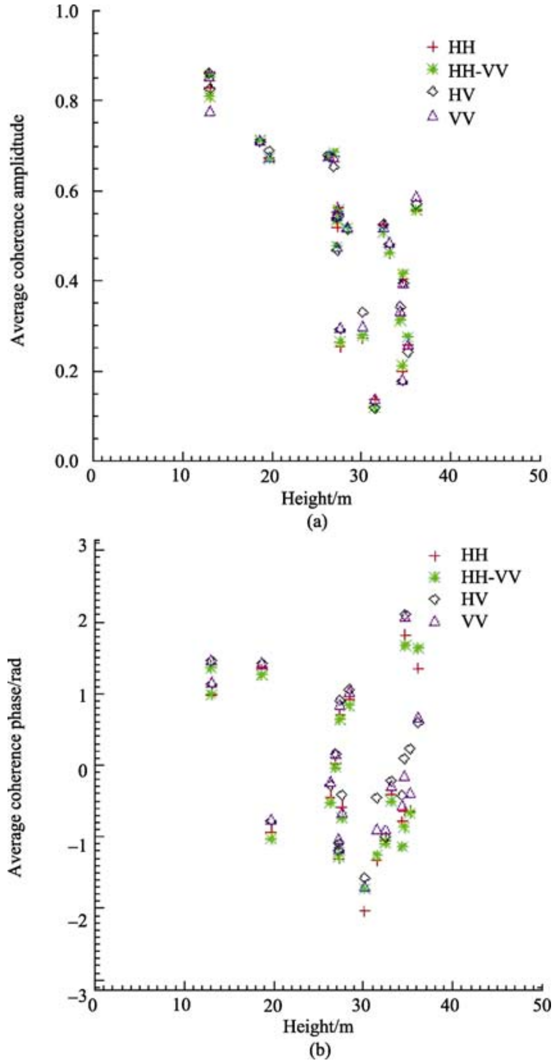

Fig. 2 Scatter diagram of different polarization interferometric coherence vs. forest height
(a) Coherence amplitude; (b) Coherence phase

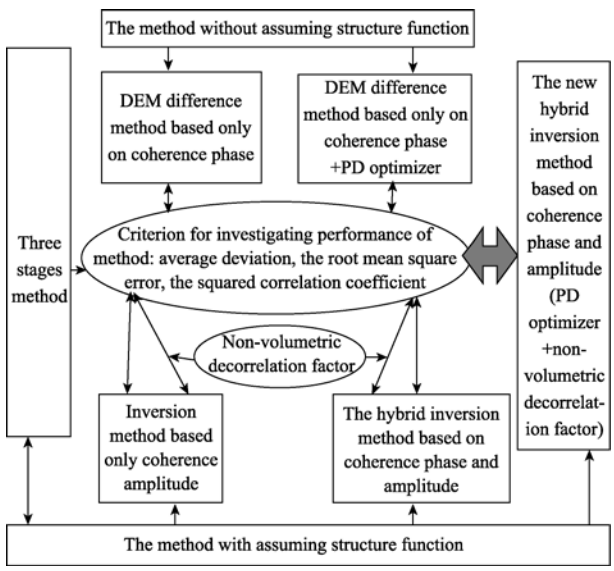

Fig. 3 Flow chart of this study

rence of HH-VV polarization is considered as γ_{w_s} . Average tree height inversed from Eq. (1) is plotted against ground measured average forest height in Fig.4(a), The performance is shown in Table 1. The forest height was significantly underestimated because the difference between coherence phase of HV and HH-VV is small. So, we naturally think of using the polarization interferometric coherence optimization algorithm to determine γ_{w_v} and γ_{w_s} and we want to know whether it is more advantageous to the separation of interferometric coherence phase centers of different scattering mechanism. Average forest height for each stands are obtained using DEM difference method with γ_{w_v} and γ_{w_s} defined by the PD polarimetric interferometric coherence optimization algorithm (Eq. (8) – (11) in Section 5), and the scatter diagram against ground measured average tree height is shown as Fig.4 (b). Although the square of correlation coefficient R^2 increased (Table 1), the tree height is still seriously underestimated. The results indicate the capability for PD interferometric coherence optimization algorithm to extract coherent component of "pure" volume scattering and "pure" surface scattering mechanism is limited.

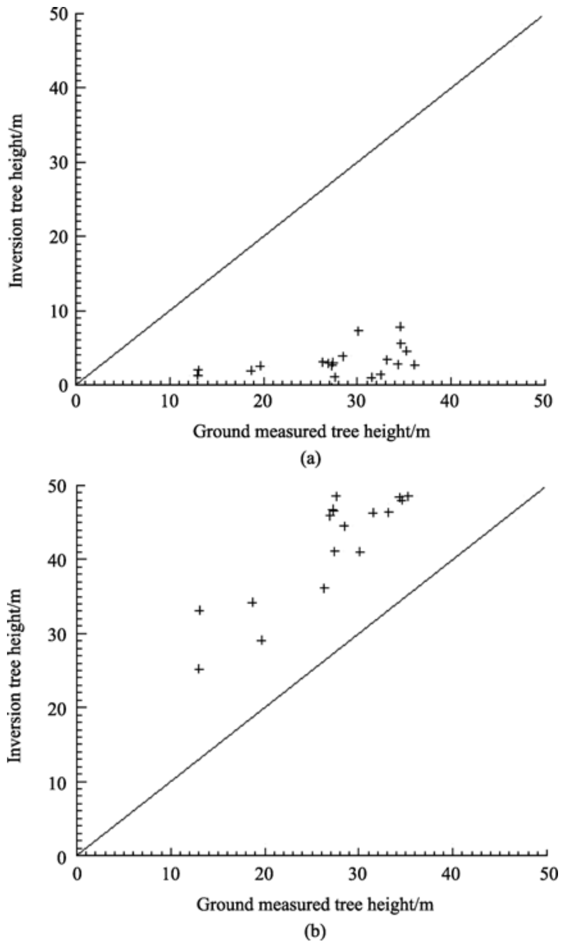

Fig. 4 Scatter diagram of average forest height inversed by DEM difference method with ground measured average forest height.
(a) Taking interferometric coherence of HV as γ_{w_v} and that of HH-VV as γ_{w_s} ; (b) γ_{w_v} and γ_{w_s} were defined by the PD polarimetric interferometric coherence optimization algorithm

Table 1 Comparison of inversion results

Inversion Method used , polarization for γ_{w_v} and γ_{w_s}	Average deviation /m	The squared correlation coefficient (R^2)	The root mean square error (RMSE) /m
DEM difference method, HV and HH-VV polarization	−24.895	0.170	25.663
DEM difference method, polarization defined by the PD optimizer	−21.988	0.503	22.633
SINC method, HV polarization	15.874	0.766	16.420
SINC method, HV polarization, non-volumetric decorrelation factor	11.878	0.849	12.923
Three stages method	8.324	0.839	8.758
The hybrid inversion method, HV and HH-VV polarization	−0.181	0.286	6.288
The hybrid inversion method, HV and HH-VV polarization, non-volumetric decorrelation factor	−2.535	0.509	5.741
the new hybrid inversion method, polarization defined by the PD optimizer	3.434	0.678	5.206
the new hybrid inversion method, polarization defined by the PD optimizer, non-volumetric decorrelation factor	0.927	0.809	3.343

4 INVERSION METHOD WITH ASSUMING STRUCTURE FUNCTION

4.1 Random volume scattering model

The RVoG model is simplified as random volume (RV) model when the ratio of effective surface to volume scattering is assumed to be zero. The corresponding coherence function is shown as Eq.(2) ,

$$\gamma_{\mathrm{v}} = \exp(\mathrm{j}\phi_0)\frac{\int_0^h \exp(2\alpha z/\cos\theta)\cdot\exp(\mathrm{j}k_z z)\mathrm{d}z}{\int_0^h \exp(2\alpha z/\cos\theta)\mathrm{d}z} \tag{2}$$

where the vertical structure function is assumed to be an exponent function; α is the mean extinction coefficient, ϕ_0 is the ground phase. Without considering the surface phase, γ_{v} is determined by two parameters, namely the height of the vegetation and its mean extinction coefficient. The relationship between the coherence amplitude, phase and the height, mean extinction coefficient is shown in Fig.5. It can be seen from Fig.5 (a) that coherence amplitude is prone to saturate when mean extinction coefficient is high, but the coherence phase is not saturated. In this case, it is a good way to use phase information for forest height inversion. When coherent phase is kept fixed, possible forest height can vary with the coherent amplitude because of the extinction coefficient difference. RV model becomes SINC function when extinction coefficient equals zero and coherence quickly decreased as the forest height increases. From Fig.5, it can be seen that in case of equal forest height, when coherent amplitude is high, surface scattering contribution is dominant due to the terrain surface scattering or the strong forest canopy attenuation, which may be distinguished by coherence phase information: it will comes from strong attenuation caused by dense vegetation if the coherence phase value is high; otherwise it will comes from the ground surface under sparse vegetation.

Adding the effect of surface scattering on the coherence in the RV model, we get the RVoG model. Some inversion methods based on the RVoG model and its simplified forms will be discussed in detail as follows.

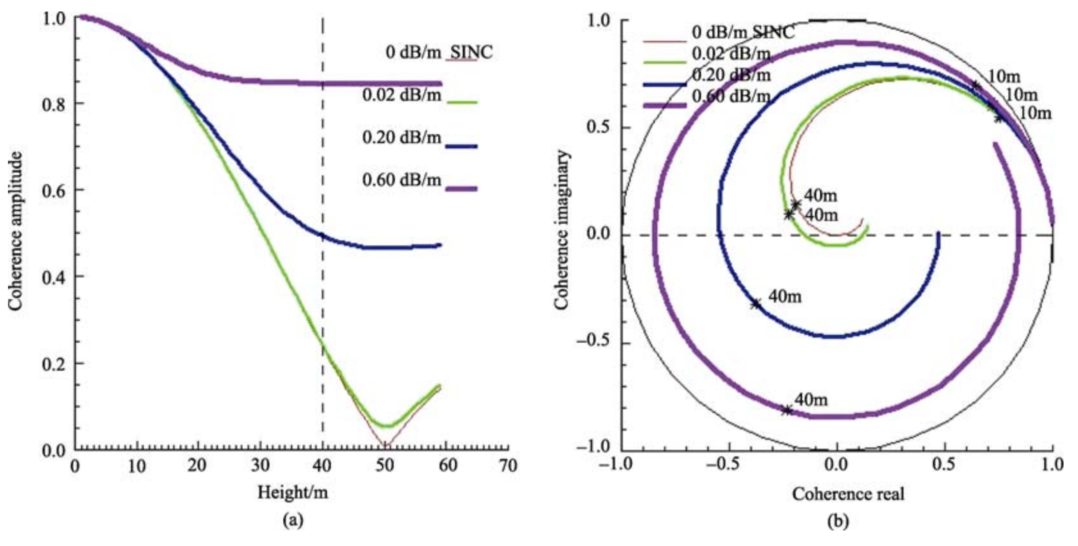

Fig. 5 Change of interferometric coherence with forest height and extinction
(a) Coherence amplitude; (b) Coherence amplitude and phase

4.2 Inversion algorithm with constant structure function

The method is based on single-layer model with one constant structure function assuming the scattering is only from a random volume. For forest height inversion, only the amplitude information is considered, while the phase and the surface backscattering are completely ignored. A polarization channel with expected low surface to volume scattering ratio (HV to HV coherence, for example) is always subjectively selected as volume coherence during the inversion. The algorithm is sensitive to forest stands with strong canopy structure variations. Big forest height estimation error is possible due to serious vertical structure variations in the canopy, Furthermore, if we set the mean extinction as zero, the model becomes a ‘‘SINC’’ function (Eq.(3)).

$$\gamma_{\mathrm{v}} = \lim_{\alpha\to 0}\left(\exp(\mathrm{j}\phi_0)\frac{\int_0^h \exp(2\alpha z/\cos\theta)\cdot\exp(\mathrm{j}k_z z)\mathrm{d}z}{\int_0^h \exp(2\alpha z/\cos\theta)\mathrm{d}z}\right) = \exp(\mathrm{j}\phi_0)\exp\left(\mathrm{j}\frac{1}{2}k_z h\right)\frac{\sin\left(\frac{1}{2}k_z h\right)}{\frac{1}{2}k_z h} \tag{3}$$

Coherence of HV to HV is also selected as γ_{v} and the forest heights of the 20 validation stands are inversed using Eq.(3). Scatter plot of the estimated forest height with the ground measured is shown in Fig.6 (a). The correlation with the ground-measured heights is good ($R^2 = 0.766$ as shown in Table 1), but the forest heights are overestimated for each validation stand. From Fig.5 (a), it can be seen that the forest height should be underestimated for the same coherence amplitude. So the overestimated problem observed may be caused by the contribution of non-volumetric related decorrelation, which should be compensated before inversion process.

For measuring vegetation through repeat-pass interferometry, there are volume decorrelation and non-volumetric related decorrelation sources (range, temporal or system decorrelation). In the RVoG-model (Eq.(6) in Section 4.3), range- and system-decorrelation affect all coherences equally and temporal decorrelation affects only the volume-coherence as shown in Eq.(4) (Mette, 2007).

$$\gamma = \gamma_{\mathrm{range}}\gamma_{\mathrm{system}}\left[\gamma_{\mathrm{temporal}}\gamma_{\mathrm{v}} + \frac{\mu}{1+\mu}\left(1-\gamma_{\mathrm{temporal}}\gamma_{\mathrm{v}}\right)\right] \tag{4}$$

$$\gamma = \gamma_{\mathrm{v}}\gamma_{\mathrm{d}} \tag{5}$$

Summarizing the ‘non-volumetric’ decorrelation in a single decorrelation factor γ_{d}, the total coherence can be expressed as Eq. (5). According to the characteristics of E-SAR system and the different effects of each kinds of non-volumetric decorrelation sources on height estimation, an average decorrelation factor (γ_{d}=0.9) was used and discussed in this study.

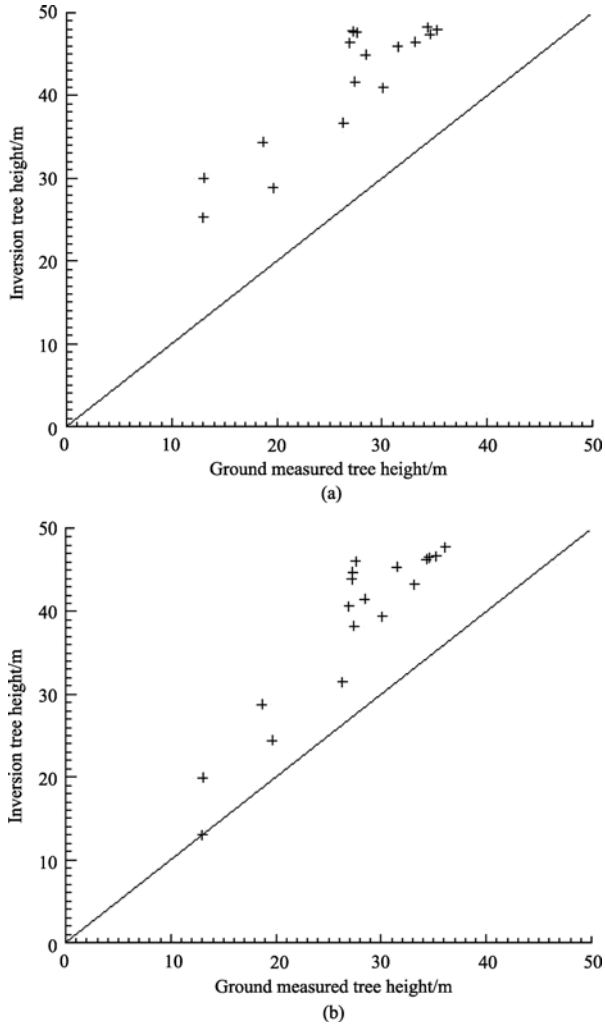

Fig. 6 Scatter diagram of average forest height by SINC inversion model with ground measured average forest height taking HV interferometric coherence as input
(a) Without non-volumetric decorrelation compensation; (b) With non-volumetric decorrelation compensation

Coherence of HV to HV polarization that was corrected through incorporating the average decorrelation factor into Eq.(5) to compensate all the non-volumetric decorrelation, is considered as γ_{v}. Then forest heights are estimated from Eq.(3) and the average height for each validation stand is computed. The inversion results are shown as scatter plot of Fig.6 (b). It is evident that the overestimated problem is solved in some degree by this way.

4.3 Inversion algorithm with extinction and ground contribution

Assuming an exponential structure function and taking the contribution of surface scattering into consideration, the RVoG model can be expressed as Eq.(6) for forest height inversion ,

$$\tilde{\gamma}(\boldsymbol{w}) = e^{i\phi_0}\left[\tilde{\gamma}_{\mathrm{v}} + \frac{\mu(\boldsymbol{w})}{1+\mu(\boldsymbol{w})}(1-\tilde{\gamma}_{\mathrm{v}})\right] \tag{6}$$

where $\mu(\boldsymbol{w})$ denotes the ground-to-volume scattering ratio being of polarization dependent. It can be seen from Eq.(6) that the complex coherence follows a straight line in the coherence unit circle which intersects the circle at two points. One of the two points corresponds to the underlying topography phase, so this point is called the true ground phase point; the "pure" volume coherence will be furthest away in distance from the true ground phase point along the line. According to this principle, Cloude and Papathanassiou (2003)developed the three-stages inversion method as the following:

(1) Using least squared error regression algorithm to fit one line to the real and imaginary components of the data, a pair of points on the unit circle that defines a line and minimizes the mean squared error (MSE) between the line and the set of coherence points are found out.

(2) Determine one of the pair points as the ground phase point using ranking order algorithm.

(3) Then, after removing the effect of surface scattering and ground topography on coherence, forest height and corresponding extinction coefficient can be estimated using one 2D look-up table (LUT).

Scatter diagram of estimated average forest height by three-stages method with ground measured average forest height is shown in Fig.7. Although the R^2 value is high, the root mean squared error (RMSE) is relative big (RMSE=8.758) and the overestimated problem is still existed.

4.4 Hybrid inversion method based on fusion of the coherence amplitude and phase information

From the above we can see that forest height estimated just from the phase information (DEM difference method) is underestimated. It is very difficult to find polarizations with phase centre exactly at the top and bottom of the vegetation layer, since polarization is " contaminated" by the volume scattering. Although coherence optimization is useful to the effective estimation of ground phase, the phase of the volume only scattering

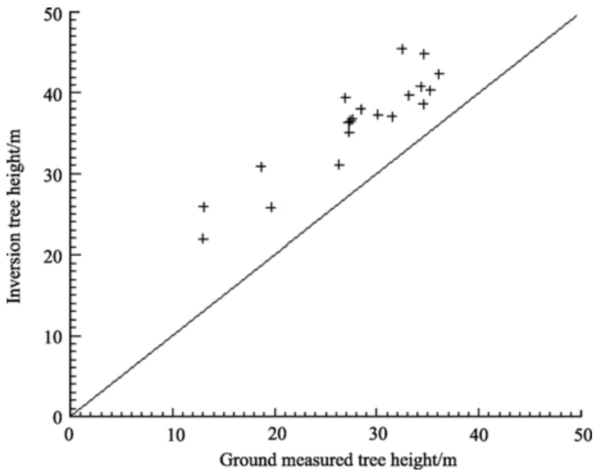

Fig. 7 Scatter diagram of estimated average forest height by three-stages method with ground measured average tree height

channel can lie anywhere between half-way and the top of the canopy layer, and hence in general this will lead to underestimated forest height (Fig. 4(b)). The simplified inversion algorithm based only on coherence amplitude information, even taking into account the impact of non-volumetric decorrelation, still overestimates the forest height (Fig. 6(b)). Therefore, it is possible to get improved inversion results by combining the two methods (Cloude, 2006). The hybrid inversion method is shown as Eq. (7).

$$h_{\mathrm{v}} = \frac{\arg(\tilde{\gamma}_{\boldsymbol{w}_{\mathrm{v}}}) - \hat{\phi}_0}{k_{\mathrm{z}}} + \varepsilon \frac{2\sin c^{-1}(|\tilde{\gamma}_{\boldsymbol{w}_{\mathrm{v}}}|)}{k_{\mathrm{z}}} \text{ where,}$$

$$\hat{\phi}_0 = \arg[\tilde{\gamma}_{\boldsymbol{w}_{\mathrm{v}}} - \tilde{\gamma}_{\boldsymbol{w}_{\mathrm{s}}}(1 - L_{\boldsymbol{w}_{\mathrm{s}}})], 0 \leqslant L_{\boldsymbol{w}_{\mathrm{s}}} \leqslant 1$$

$$AL^2_{\boldsymbol{w}_{\mathrm{s}}} + BL_{\boldsymbol{w}_{\mathrm{s}}} + C = 0 \Rightarrow L_{\boldsymbol{w}_{\mathrm{s}}} = \frac{-B - \sqrt{B^2 - 4AC}}{2A}$$

$$\begin{aligned} A &= \left|\tilde{\gamma}_{\boldsymbol{w}_{\mathrm{s}}}\right|^2 - 1 \\ B &= 2\,\mathrm{Re}((\tilde{\gamma}_{\boldsymbol{w}_{\mathrm{v}}} - \tilde{\gamma}_{\boldsymbol{w}_{\mathrm{s}}})\tilde{\gamma}^*_{\boldsymbol{w}_{\mathrm{s}}}) \\ C &= \left|\tilde{\gamma}_{\boldsymbol{w}_{\mathrm{v}}} - \tilde{\gamma}_{\boldsymbol{w}_{\mathrm{s}}}\right|^2 \end{aligned} \qquad (7)$$

The idea of the method is that as the phase centre separation increases, the effective volume depth decreases (as the structure function becomes more localized near the top of the layer), hence the level of volume decorrelation will decrease. SINC coherence function is used to make up the phenomenon of "compression" at the top of vegetation which is always happen with phase only inversion method. ε can be taken different value due to different structure function. There are two important special cases: Firstly, the medium has a uniform structure function (extinction is zero), then the first term will give half the height or $\frac{1}{2}k_{\mathrm{z}}h_{\mathrm{v}}$, and we can know from Eq.(3) that the second term will also obtain half the true height and yield $\frac{1}{2}k_{\mathrm{z}}h_{\mathrm{v}}$, therefore ε is set as 1/2; Secondly, to the opposite extreme of infinite extinction, the structure function in the volume channel is localized near the top of the layer, then the first term will give $k_z h_{\mathrm{v}}$ and the second term will approach zero, this means ε=0 is the correct choice. So the inversion method will provide a reasonable estimate for arbitrary structure functions between these two extremes and ε value is proposed to be 0.4 as a suitable compromise for height estimation in varying forest density and structure environments (Cloude, 2006).

Coherence of HV to HV is considered as $\gamma_{\boldsymbol{w}_{\mathrm{v}}}$, coherence of HH-VV to HH-VV is used as $\gamma_{\boldsymbol{w}_{\mathrm{s}}}$, are inputted to Eq.(7) and scatter plot is shown in Fig.8(a). R^2 is low. Even using the average decorrelation factor by the same way in section 4.2, R^2 is still low, and that indicate the two polarization channels selected from the physical mechanism point is not dominant by "pure" volume scattering and surface scattering respectively, with phase centers are furthest between.

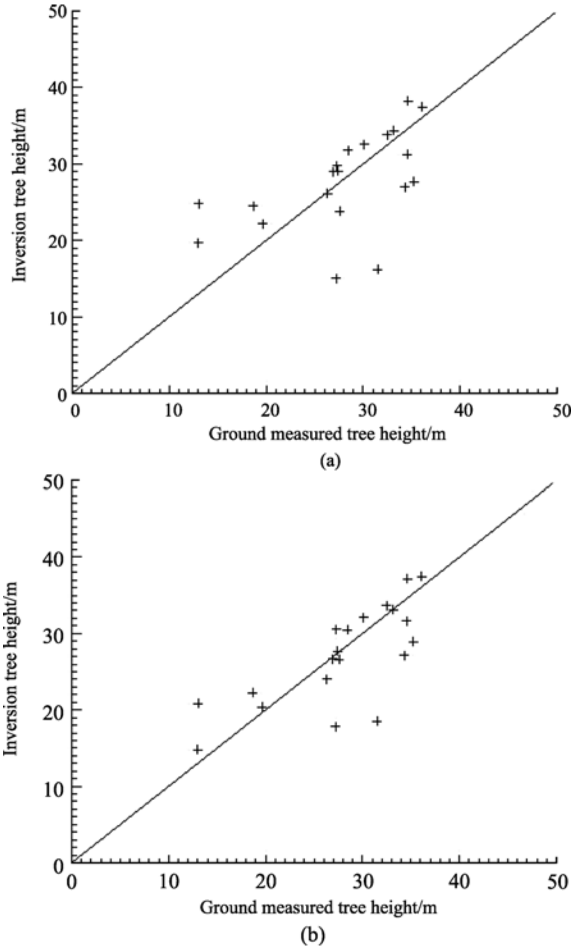

Fig. 8 The scatter diagram of estimated average forest height by the hybrid inversion method with ground measured average forest height
(a) Without non-volumetric decorrelation compensation; (b) With non-volumetric decorrelation compensation

5 IMPROVEMENT OF HYBRID INVERSION METHOD

The increasing phase center separation by interferometric coherence optimization method is useful for choosing polarization channels dominated by "pure" volume scattering and surface scattering respectively. In this study, Phase Diversity (PD) interferometric coherence optimization method is used for the purpose, which is based on maximization of the separation of the phase center of the POLInSAR coherence.

The basic idea of PD method is to find the eigenvectors (Eq.(9)) that maximize the cotangent of the phase of the complex coherence (Eq.(8)). Ω_{12}, elements of the matrix T (Eq.(10)), contains polarimetric and interferometric information.

$$\cot(\angle\tilde{\gamma}) = \frac{\mathrm{Re}\{\tilde{\gamma}\}}{\mathrm{Im}\{\tilde{\gamma}\}} = \frac{\boldsymbol{w}^*(\Omega_{12}+\Omega^*{}_{12})\boldsymbol{w}}{\boldsymbol{w}^*[-j(\Omega_{12}-\Omega^*{}_{12})]\boldsymbol{w}} \tag{8}$$

$(\hat{\Omega}_{12}+\hat{\Omega}^*_{12})\boldsymbol{w} = -j\lambda(\hat{\Omega}_{12}+\hat{\Omega}^*_{12})\boldsymbol{w}$, where

$$\hat{\Omega}_{12} = \Omega_{12}\mathrm{e}^{j(\frac{\pi}{2}-\angle tr(\Omega_{12}))} \tag{9}$$

$$T \leqslant \begin{bmatrix}\boldsymbol{k}_1\\ \boldsymbol{k}_2\end{bmatrix}\begin{bmatrix}\boldsymbol{k}_1^{*\mathrm{T}} & \boldsymbol{k}_2^{*\mathrm{T}}\end{bmatrix} \geqslant \begin{bmatrix}[T_{11}] & [\Omega_{12}] \\ [\Omega_{12}]^{*\mathrm{T}} & [T_{22}]\end{bmatrix} \tag{10}$$

where $\boldsymbol{k} = \frac{1}{\sqrt{2}}\begin{bmatrix}S_{\mathrm{HH}}+S_{\mathrm{VV}}\\ S_{\mathrm{HH}}-S_{\mathrm{VV}}\\ 2S_{\mathrm{HV}}\end{bmatrix}$, <> represents the multi–looking operator, the subscripts 1, 2 denote the measurement of the two ends of spatial baseline respectively.

Element in (0,0) of 3×3 eigenvectors matrix from Eq.(9) is the eigenvector corresponding to the largest eigenvalue that is associated with highest phase center where "pure" volume scattering is dominant. And element in (3, 3), is the eigenvector corresponding to the smallest eigenvalue that is associated with lowest phase center where "pure" surface scattering is dominant.

The optimum coherence values obtained from Eq.(11) using the two eigenvector are considered as $\gamma_{\boldsymbol{w}_\mathrm{v}}$ and $\gamma_{\boldsymbol{w}_\mathrm{s}}$ respectively, and inputted to Eq.(7). Thus forest heights estimated for 20 validation stands is used to plot against ground measured average forest height in Fig. 9(a). It can be seen that the general performance of the method is good (Table 1), but the overestimated problem still exists in some degree. By taking into account the impact of non-volumetric decorrelation, the general performance has been further improved.

$$\tilde{\gamma} = \frac{\boldsymbol{w}^{*\mathrm{T}}\Omega_{12}\boldsymbol{w}}{\boldsymbol{w}^{*\mathrm{T}}T\boldsymbol{w}} \quad \text{where } T=(T_{11}+T_{22})/2 \tag{11}$$

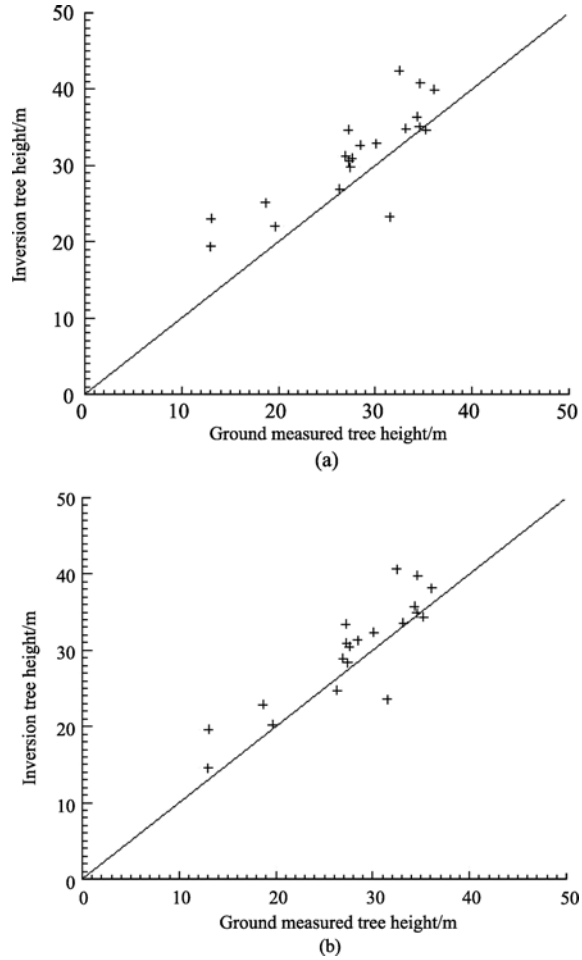

Fig. 9 Scatter diagram of estimated average forest height by the new hybrid inversion method with ground measured average forest height
(a) Without non-volumetric decorrelation compensation; (b) With non-volumetric decorrelation compensation

The forest height inversion performance of the methods involved in the paper was summarized in Table 1. DEM difference method is the worst with largest RMSE and lowest R^2. $\gamma_{\boldsymbol{w}_\mathrm{v}}$ and $\gamma_{\boldsymbol{w}_\mathrm{s}}$ determined by PD interferometric coherence optimization method was used in DEM method to improve R^2 to 0.503. Instead of using coherence of HV and HH-VV, if the optimum coherence values obtained by PD is used in the hybrid inversion method based on fusion of the coherence amplitude and phase information, the RMSE can be reduced from 6.288m to 5.206m and R^2 is improved from 0.286 to 0.678, which indicates PD can separate effectively the phase center of coherence. Further considering the compensation of non- volumetric decorrelation, the RMSE is reduced to 3.343m, which is the smallest of all the methods, while R^2 is increased to 0.809.

It is shown in Fig.10 that forest height profile along the azimuth direction (a straight line of column 278 in the image shown in Fig.1)of three inversion algorithms involved in the paper. It can be seen that the inversion method developed in the paper (corresponding to the green line) can significantly improve the performance of inversion.

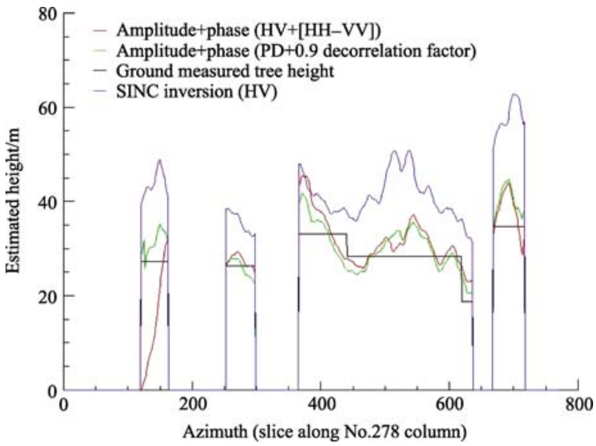

Fig. 10 Forest height profile along the azimuth direction (a straight line of column 278 in the image shown in Fig.1)of three inversion algorithms.

6 CONCLUSIONS

Several available forest height inversion methods for POLInSAR data were investigated and compared using repeat pass E-SAR L band polarimetric SAR interferometry data and the corresponding ground measured forest stand height. The results show that: (1) the overestimated problem for forest height caused by non-volumetric decorrelation can be solved in some degree by taking into account the average decorrelation factor γ_d. (2) PD interferometric coherence optimization method can separate effectively the phase center of coherence for different scattering mechanism, and can be used for improving the inversion performance in the DEM difference method and the hybrid inversion method. (3) Although the hybrid inversion method is simple, however it considers comprehensively the underestimated and overestimated problem associated with inversion method based only on the coherent phase or the amplitude respectively, higher accuracy for forest height estimation can be obtained if some ground true information available. The paper proposed one improved inversion method by incorporating interferometric coherence optimization and compensation of non-volumetric decorrelation into the hybrid inversion method, the validation result shows that the general performance of this method is superior to the others.

Acknowledgements: The experimental data used in the study are provided under the contract of the Dragon 2 program between the MOST and ESA.

REFERENCES

Chen E X, Li Z Y, Pang Y and Tian X. 2007. Polarimetric synthetic aperture radar interferometry based mean tree height extraction technique. *Scientia Silvae Sinicae*, **43**(4): 66—71

Chen E X, Li Z Y, Cloude S R, Papathanassiou K P and Pottier E. 2008. Comparison of methods to derive forest height from polarimetric SAR interferometry. DRAGON-1 Final Symposium, Beijing

Chen X, Zhang H and Wang C. 2008. Vegetation parameter extraction using dual baseline polarimetric SAR interferometry data. *Journal of Electronics & Information Technology*, **30**(12): 2858—2861

Cloude S R and Papathanassiou K P. 1998. Polarimetric SAR interferometry. *IEEE Transactions on Geoscience and Remote Sensing*, **36**(5): 1551—1565

Cloude S R and Papathanassiou K P. 2003. Three-stage inversion process for polarimetric SAR interferometry. *IEEE Proc. Radar Sonar Navig.*, **150**(3): 125—134

Cloude S R. 2006. Polarization coherence tomography. *Radio Science*, **41**(4): RS4017.1—RS4017.27

Hajnsek I, Kugler F, Lee S-K and Papathanassiou K P. 2009. Tropical forest parameter estimation by means of PolInSAR: The INDREX-II campaign. *IEEE Transactions on Geoscience and Remote Sensing*, **47**(2): 481—493

Li X W, Guo H D, Li Z and Wang C L. 2005. Method study of vegetation height estimation using SIR-C dual frequency polarimetric SAR interferometry data. *Chinese High Technology Letters*, **15**(7): 79—84

Mette T, Kugler F, Papathanassiou K P and Hajnsek I. 2006. Forest and the random volume over ground-nature and effect of 3 possible error types. Proceedings of 6th European Conference on Synthetic Aperture Radar (EUSAR 2006). Germany: VDE Verlag GmbH

Mette T. 2007. Forest Biomass Estimation from Polarimetric SAR Interferometry. Munich: Munich University of Technology

Neumann M, Ferro–Famil L and Reigber A. 2009. Improvement of vegetation parameter retrieval from polarimetric sar interferometry using a simple polarimetric scattering model. POLInSAR'2009 Conference

Tabb M, Orrey J, Flynn T and Carande R. 2002. Phase diversity: a decomposition for vegetation parameter estimation using polarimetric SAR interferometry. Proceedings of 4th European Synthetic Aperture Radar Conference (EUSAR 2002). Cologne, Germany

Wu Y R, Hong W and Wang Y P. 2007. The current status and implications of polarimetric SAR interferometry. *Journal of Electronics & Information Technology*, **29**(5): 1258—1262

Yang L, Zhao Y J and Wang Z G. 2007. Polarimetric interferometric SAR data analysis based on TLS-ESPRIT of joint estimation of phase and power. *Acta Geodaetica Et Cartographica Sinica*. **36**(2): 163—168

Zhou G Y, Xiong T, Yang J and Zhang W J. 2008. Forest height inversion based on polarimetric SAR interferometry. 2008 9th International Conference on Signal Processing. USA: IEEE

极化干涉 SAR 森林高度反演方法研究

罗环敏[1], 陈尔学[2], 程 建[3], 李小文[1,4]

1. 电子科技大学地表空间信息技术研究所, 成都 610054;
2. 中国林业科学研究院资源信息研究所, 北京 100091;
3. 电子科技大学电子工程学院, 成都 610054;
4. 北京师范大学地理学与遥感科学学院, 北京 100875

摘 要: 在分析随机体散射体/地表二层(RVoG)散射模型的基础上, 利用德国宇航局机载 SAR 系统(ESAR)获取的 POLInSAR 数据和森林高度地面观测数据, 对多种已有的森林高度反演模型进行了比较评价, 从物理机制上对试验结果进行了分析、解释, 进而发展了一种基于极化相干优化和非体散射去相干补偿的综合反演方法, 实验结果表明, 基于该方法的树高反演效果总体上优于其他方法。

关键词: 极化干涉 SAR, 极化相干优化, 随机体散射体/地表二层(RVoG)散射模型, 森林高度, 非体散射去相干

中图分类号: TP722.6/S7 **文献标识码:** A

引用格式: 罗环敏, 陈尔学, 程 建, 李小文. 2010. 极化干涉 SAR 森林高度反演方法研究. 遥感学报, **14**(4): 806—821
Luo H M, Chen E X, Cheng J and Li X W. 2010. Forest height estimation methods using polarimetric SAR interferometry. *Journal of Remote Sensing*. **14**(4): 806—821

1 引 言

森林高度是林业资源信息中一个重要参数, 同时也是森林蓄积量和森林地上生物量估计等模型的一个重要输入参数。随着遥感技术的发展, 植被反演技术也日益成为 SAR 技术研究领域的一个热点, 其中极化干涉(POLInSAR)技术组合干涉对植被结构组分的位置和垂直分布敏感的优势和极化信息对植被结构组分形状和方位敏感的优点, 成为植被高度反演技术的一种关键技术(吴一戎等, 2007)。Cloude 和 Papathanassiou(2003)利用描述植被高度和极化相干之间关系的随机体散射体/地表二层散射(RVoG)模型, 提出单基线 POLInSAR 森林高度三阶段反演方法。Neumman 等(2009)结合极化分解和 RVoG 模型, 提出二分量极化干涉森林参数反演模型, 并利用 Nelder-Mead 单纯形优化方法, 提高森林高度反演精度。Hajnsek 等(2009)利用印度尼西亚热带森林的 P, L, X 波段机载 POLInSAR 数据, 对森林高度反演中时间解相关、地表等因素的影响进行了讨论。

陈尔学等(2007, 2008)利用新疆和田的 SIR-C/X SAR 极化干涉数据, 提取了森林植被的高度信息, 并结合光学影像对产生的误差源进行了定性分析; 利用同一实验区的 ESAR 数据和地面实测数据对常用的反演算法进行了定量评价。一些学者(杨磊等, 2007; Zhou 等, 2008)基于同一像元中不同散射机制相位中心之间的差异, 利用 ESPRIT 算法, 提取优势相位用于森林高度计算, 结果显示计算效率有所提高, 但对反演精度的改善有限。另外, 李新武等(2005), 陈曦等(2008), 也进行了相关研究, 他们在观察空间中, 从增加基线信息或频率信息的角度研究了提高森林高度反演精度的方法。

本文在分析已有的反演算法的基础上, 根据极化信号和植被相互作用的物理机制, 采用 Phase Diversity(PD)极化相干优化方法(Tabb 等, 2002)确定地表散射相位和冠层散射相位中心, 结合相干幅度和相位信息, 基于 RVoG 模型提取森林高度, 用地面调查数据对结果进行验证, 并和其他反演方法进行精度对比, 以探索和发展效果更好的反演方法。

收稿日期: 2009-09-11; 修订日期: 2010-02-01
基金项目: 国家重点基础研究计划(973 计划)(编号: 2007CB714404)。

第一作者简介: 罗环敏(1972—), 男, 电子科技大学地表空间信息技术研究所在读博士, 目前主要从事极化干涉 SAR 植被信息提取方面的研究工作。E-mail: Lhm123345@qq.com。

2 试验区及数据介绍

用的数据是德国宇航局(DLR)利用 ESAR 机载系统，在德国南部的特劳斯坦试验场获取的 L 波段重复轨极化干涉 SAR 数据。航摄飞行高度约为 3km，干涉水平基线为 5m，时间基线为 20min。近距入射角为 25°，远距达 60°。距离向分辨率为 1.5m，方位向分辨率为 3m。

该试验区海拔在 600—650 m，地形平坦。地物类型主要包括城镇、农田、森林和牧场。试验区主要优势树种为云杉、山毛榉和冷杉。与飞行试验近同步，对 20 个林分进行了详细的样地抽样调查，最终估计得到每个林分的平均优势高(h_v，每公顷林分最高的 100 株树的平均高)。这 20 个林分大部分是混交林，树高最高达 40m，生物量高达 450t/hm^2。

干涉 SAR 主影像的 PAULI 分解结果的 RGB 彩色组合显示见图 1，可以看出，在植被区，用绿色表示反映体散射的 HV 分量占主导作用。但要注意，在植被区域的一些周边，有强烈的二次散射。

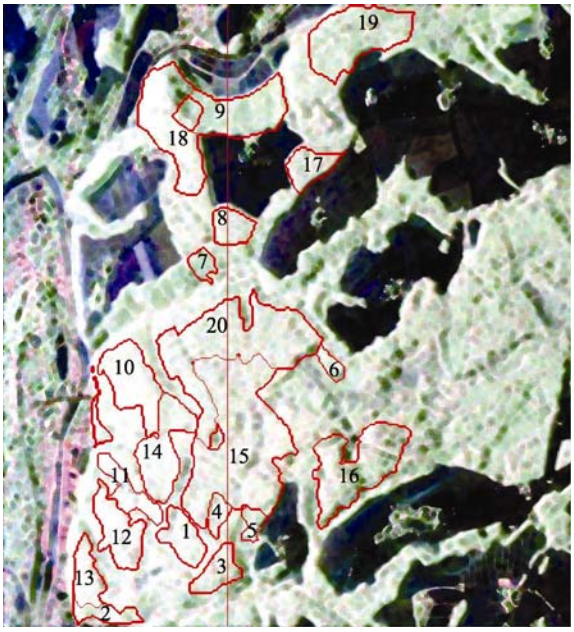

图 1 试验区极化数据的 PAULI 分解结果图

提取出 20 个地面实测林分(如图 1 中多边形所示)的 4 种极化方式(HH、HV、VV 和 HH-VV)的平均相干幅度、平均相干相位，分别与林分平均高绘制散点分布图(图 2)，可以看出，这 4 种极化方式的平均干涉相位相互之间差别不大(图 2(b))；4 种极化方式的平均相干幅度与林分高度有较高的相关性，但是，各极化方式之间的差别不大(图 2(a))。这些现象说明自然条件下，森林极化相干是多种散射机制和因素的综合贡献，仅基于散射机制分离的树高反演算法必然存在较大误差。为了提高反演精度，提出了多种反演模型。本文基于该试验区数据，对多种森林高度反演模型进行了定量分析评价，采用的技术路线见图 3。

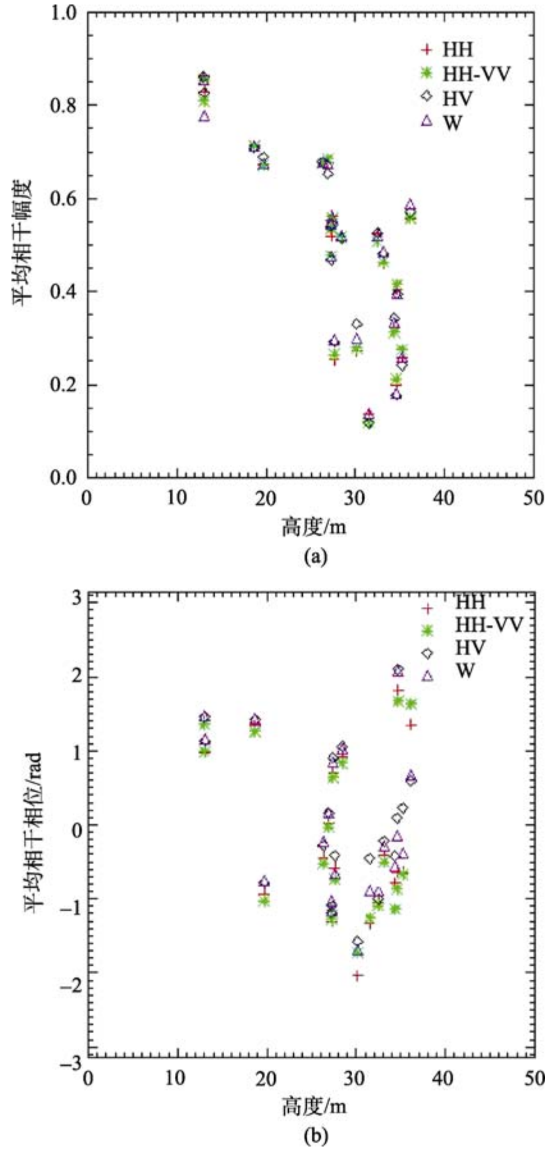

图 2 不同极化相干幅度(a)及相位(b)随森林高度的变化散点图

3 无结构函数假设的反演法

该方法最早被称为 DEM 差值法(Cloude & Papathanassiou, 1998)，严格来讲，称为 DSM 差值法更合适。它不对植被的结构函数做假设，简单地认为冠层顶部“纯”体散射占主导作用的相干相位减去树

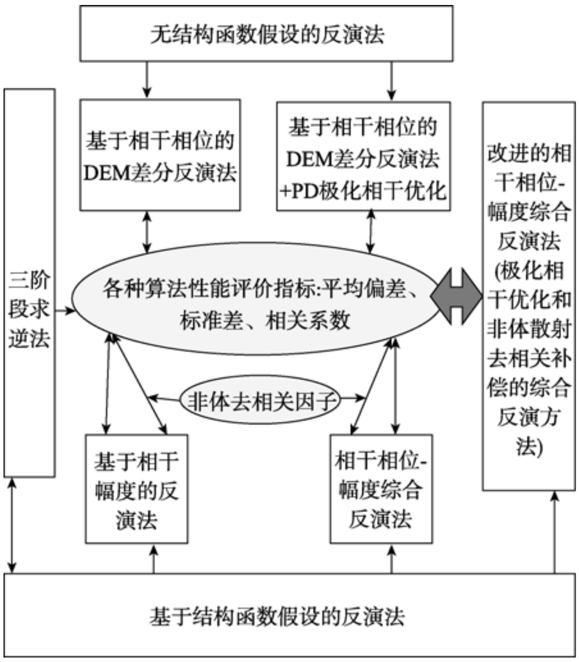

图 3 研究技术路线

冠下地表散射占主导作用的相干相位，再除以有效波数，就是植被的高度，见式(1)，$h_v = \dfrac{\arg(\gamma_{w_v}) - \arg(\gamma_{w_s})}{k_z}$，其中

$$k_z = \frac{4\pi\Delta\theta}{\lambda\sin\theta} \tag{1}$$

式中，k_z是有效波数，用于将相位差转换成垂直高度；θ为入射角；$\Delta\theta$为干涉影像对入射角差异；γ_{w_v}表示植被冠层“纯体散射”机制的干涉相干，γ_{w_s}表示树冠覆盖下的地表“纯表面散射”机制的干涉相干。若选择HV极化计算γ_{w_v}，HH-VV极化计算γ_{w_s}。按式(1)求得的林分平均高度和实测平均高度的散点图见图4(a)，树高的估计结果(表1)明显偏低，原因是HV极化与HH-VV极化的干涉相干相位本来就没有多大差别(图2(b))。利用极化干涉相干优化算法得到的相干分量确定γ_{w_v}和γ_{w_s}是否更有利于不同散射机制干涉相位中心的分离?图4(b)给出了由PD极化相干优化算法确定的γ_{w_v}和γ_{w_s}(见式(8)-(11))，利用DEM差值法得到的反演树高与实测树高的散点分布图。就该试验区林分，虽然相关系数平方R^2有所提高(表1)，但总体仍然严重低估树高，表明PD极化相干优化算法对纯体散射和纯表面散射相干分量的分离能力是有限的。

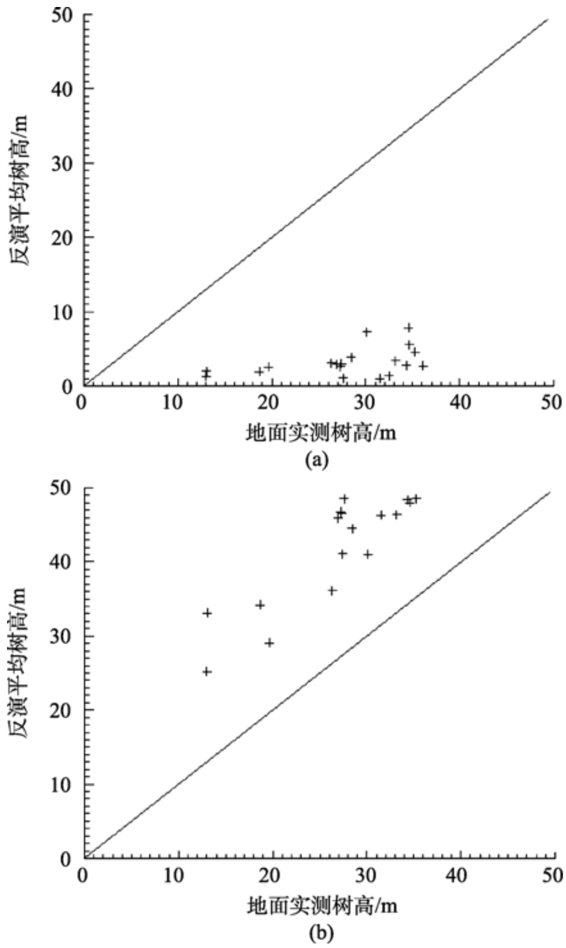

图 4 DEM差值法反演平均树高和地面实测平均树高的散点图

(a) 以HV和HH-VV极化的干涉相干分别作为γ_{w_v}和γ_{w_s}；(b) 基于PD极化相干优化算法确定的γ_{w_v}和γ_{w_s}

表 1 反演结果比较

反演模型和方法	平均偏差/m	相关系数平方/R^2	均方根误差RMSE/m
DEM差分法, HV、HH-VV极化	−24.895	0.170	25.663
DEM差分法, PD极化相干优化	−21.988	0.503	22.633
SINC反演法, HV极化	15.874	0.766	16.420
SINC反演法, HV极化, 非体去相干因子	11.878	0.849	12.923
三阶段反演法	8.324	0.839	8.758
相干幅度、相位组合反演法, HV、HH-VV极化	−0.181	0.286	6.288
相干幅度、相位组合反演法, HV、HH-VV极化, 非体去相干因子	−2.535	0.509	5.741
相干幅度、相位组合反演法, PD极化相干优化	3.434	0.678	5.206
相干幅度、相位组合反演法, PD极化相干优化, 非体去相干因子	0.927	0.809	3.343

4 基于结构函数假设的反演法

4.1 随机体散射(RV)模型

若 RVoG 模型不考虑地面散射情况, 就得到 RV 模型。该模型认为在垂直方向, 结构函数是指数形式, 相干函数如式(2)。

$$\gamma_{\mathrm{v}}=\exp(\mathrm{j}\phi_0)\frac{\int_0^h \exp(2\alpha z/\cos\theta).\exp(\mathrm{j}k_z z)\mathrm{d}z}{\int_0^h \exp(2\alpha z/\cos\theta)\mathrm{d}z} \tag{2}$$

式中, α是衰减系数, ϕ_0 是地表相位。在不考虑地表相位的情况下, γ_{v} 是高度和衰减系数的函数, 其幅度和相位随着高度、衰减系数的变化关系如图 5。可以看出, 衰减系数比较大时, 干涉相干幅度容易出现饱和现象(图 5(a)), 而此时的相位并没有饱和(图 5(b)), 所以, 这种情况下利用相位信息提取高度是一个很好的途径; 在干涉相干相位相同时, 衰减系数的差异和高度的变化, 体现在相干幅度信息中; 在衰减系数为 0 时, RV 模型就成了 SINC 函数, 此时, 随着高度的增加, 相干迅速减少, 从图 5(a)和图 5(b)可以看到。在树高相同的情况下, 当干涉相干幅度值很大时, 表面散射占主导地位, 这是由地表散或强烈的衰减引起的, 可由相位信息对二者加以区别: 如果干涉相位很大, 则是由浓密植被的强烈衰减引起的, 否则就是由低矮稀疏植被下层的地表表面散射引起的。

若在 RV 模型中加入地表散射对相干的影响, 则就是 RVoG 模型。学者们已基于 RVoG 模型及其简化形式发展了多种反演算法, 下面将分别加以介绍和比较评价。

4.2 均匀结构函数的反演方法

该方法基于均匀结构函数假设的单层模型, 即把所有的散射看成一层体散射, 只关心幅度信息, 忽略相位信息和地面散射的影响。这种假设, 对于植被结构变化特别是冠层变化大的林分会产生大的反演误差。进一步假设平均衰减系数为 0, 这时的干涉相干函数就成了一个 SINC 函数(式(3))。

$$\begin{aligned}\gamma_{\mathrm{v}}&=\lim_{\alpha\to 0}\left(\exp(\mathrm{j}\phi_0)\frac{\int_0^h \exp(2\alpha z/\cos\theta).\exp(\mathrm{j}k_z z)\mathrm{d}z}{\int_0^h \exp(2\alpha z/\cos\theta)\mathrm{d}z}\right)\\&=\exp(\mathrm{j}\phi_0)\exp\left(\mathrm{j}\frac{1}{2}k_z h\right)\frac{\sin\left(\frac{1}{2}k_z h\right)}{\frac{1}{2}k_z h}\end{aligned} \tag{3}$$

选择 HV 极化的干涉相干为γ_{v}, 利用 SINC 模型(3)求得的林分高度和实测高度的散点图如图 6(a)所示, 反演结果与实测数据的 R^2 为 0.766(表 1), 但对每个林分都产生了高估。从图 5(a)可以看出, 当相干幅度一定时, SINC 函数估计的高度应该偏低, 高估现象说明干涉相干存在非体散射去相干的影响, 在反演前应该对非体散射去相干进行适当补偿。

对于像该试验区这样通过重复飞行进行干涉测量的模式, 森林植被的干涉相干是体散射去相干、距离向去相干、时间去相干和系统去相干等的综合, 其中距离和系统去相干影响总的干涉相干, 而时间去相干只影响体散射去相干(Mette, 2007), 如式(4)。

$$\gamma=\gamma_{\mathrm{range}}\gamma_{\mathrm{system}}\left[\gamma_{\mathrm{temporal}}\gamma_{\mathrm{v}}+\frac{\mu}{1+\mu}(1-\gamma_{\mathrm{temporal}}\gamma_{\mathrm{v}})\right] \tag{4}$$

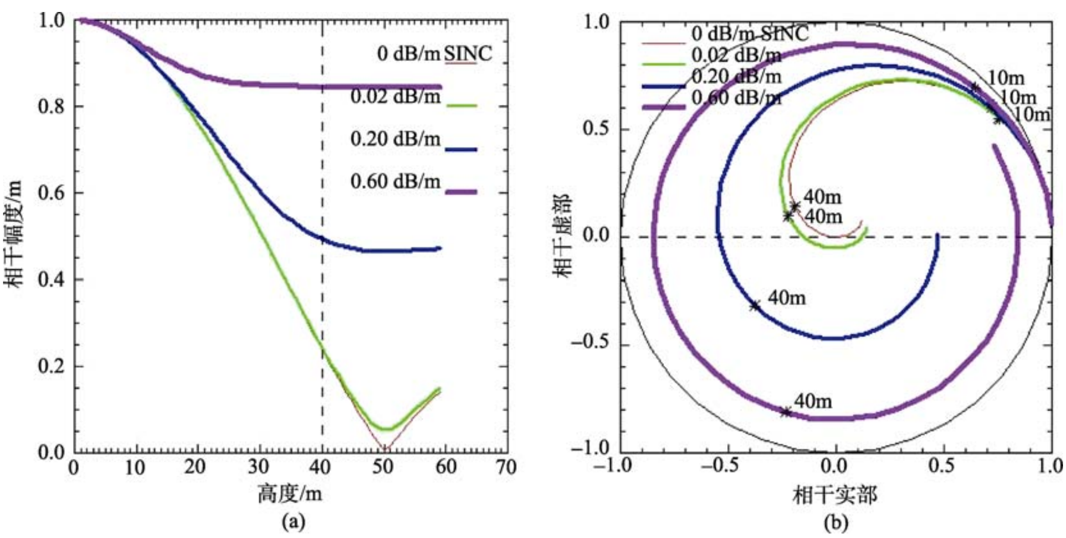

图 5 干涉相干的幅度(a) 相位(b) 与树高及衰减系数的关系

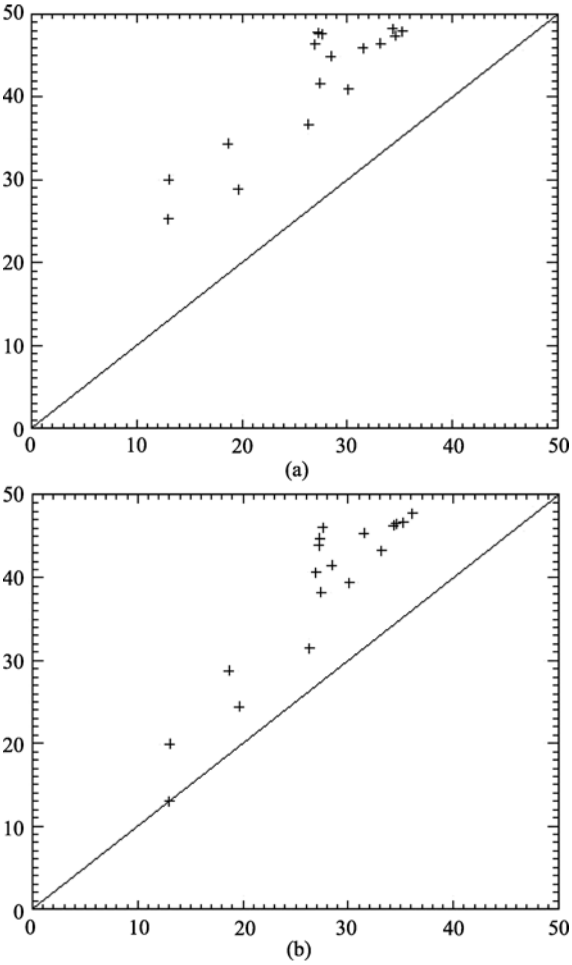

图 6　SINC 反演法估测平均树高和地面实测平均树高的散点图(采用 HV 极化干涉相干进行反演)
(a) 未进行非体散射去相干补偿; (b) 进行了非体散射去相干补偿

该式是利用 RVoG 模型(式 6)表示的。若将非体散射去相干的综合影响用一个因子γ_d表示，则总的干涉相干γ可表示为式(5)。

$$\gamma=\gamma_v\gamma_d \tag{5}$$

根据 E-SAR 系统的特点和非体散射去相干对森林高度估计精度的不同影响(Mette 等, 2006; Mette, 2007)，文中采用γ_d=0.9 对干涉相干进行补偿。

图 6(b)是对 HV 极化相干系数先施加γ_d=0.9 的非体散射去相干影响补偿得到γ_v，再利用式(3)进行反演的结果，显然高估的现象得到了一定的修正(表 1)。

4.3　基于 RVoG 模型的反演算法

RVoG 模型假设相干函数如式(6)，

$$\tilde{\gamma}(\boldsymbol{w})=e^{i\phi_0}\left[\tilde{\gamma}_v+\frac{\mu(\boldsymbol{w})}{1+\mu(\boldsymbol{w})}(1-\tilde{\gamma}_v)\right] \tag{6}$$

认为在植被垂直方向上，结构函数呈指数规律衰减，同时考虑了林下地形表面散射的影响。$\mu(\boldsymbol{w})$是极化相关的地体辐射比，由式(6)可以看出，在复平面上，复干涉相干分布在一条直线上，直线和单位圆的交点之一就是地面点，体散射相干与地相位点的距离最远。基于该原理, Cloude & Papathanassiou(2003)提出了三阶段反演算法:

(1) 最小均方线性拟合，在复平面单位圆上找到一对点,其构成的线与其他相干点的距离平方差最小。

(2) 在这一对点中，确定一个点为地表点。

(3) 去除地表相位影响，通过查找表法求得森林高度和衰减系数。

基于三阶段反演法得到的结果和实测数据的散点图如图 7。R^2 较高，但 RMSE 为 8.758(表 1)，仍有高估现象。

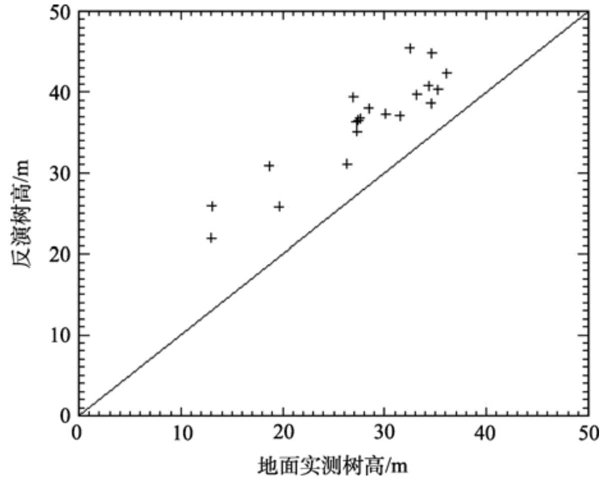

图 7　三阶段反演法求的平均树高和地面实测平均树高的散点图

4.4　相干相位-幅度综合反演法

由上文可知，单纯从相位信息估计植被高度会出现低估(DEM 差值法)问题，因为由于极化受到“污染”，找到相位中心刚好在冠层顶部和地面的极化很难。虽然相干优化可以对地形相位进行有效估计，但其估计的植被冠层相位中心点，仍然在冠层顶部和植被高度一半之间波动，所以仍会低估林分高度(图 4(b))。而单纯地用干涉相干幅度反演(SINC 反演法)，即使考虑非体去相干的影响，仍会高估林分高度(图 6(b))。因此，可以将二者综合起来，在用干涉相位信息估计的基础上，再加上基于干涉相干幅度的估测结果作为对低估结果的修正(Cloude, 2006)，如式(7)所示。

$$h_v=\frac{\arg(\tilde{\gamma}_{w_v})-\hat{\phi}_0}{k_z}+\varepsilon\frac{2\,\mathrm{sinc}^{-1}(|\tilde{\gamma}_{w_v}|)}{k_z}$$ 其中

$$\hat{\phi}_0=\arg[\tilde{\gamma}_{\boldsymbol{w}_{\mathrm{v}}}-\tilde{\gamma}_{\boldsymbol{w}_{\mathrm{s}}}(1-L_{\boldsymbol{w}_{\mathrm{s}}})],0\leqslant L_{\boldsymbol{w}_{\mathrm{s}}}\leqslant 1$$

$$AL^2_{\boldsymbol{w}_{\mathrm{s}}}+BL_{\boldsymbol{w}_{\mathrm{s}}}+C=0\Rightarrow L_{\boldsymbol{w}_{\mathrm{s}}}=\frac{-B-\sqrt{B^2-4AC}}{2A}$$

$$\begin{aligned}A&=\left|\tilde{\gamma}_{\boldsymbol{w}_{\mathrm{s}}}\right|^2-1\\B&=2\,\mathrm{Re}((\tilde{\gamma}_{\boldsymbol{w}_{\mathrm{v}}}-\tilde{\gamma}_{\boldsymbol{w}_{\mathrm{s}}})\tilde{\gamma}^*_{\boldsymbol{w}_{\mathrm{s}}})\\C&=\left|\tilde{\gamma}_{\boldsymbol{w}_{\mathrm{v}}}-\tilde{\gamma}_{\boldsymbol{w}_{\mathrm{s}}}\right|^2\end{aligned}\tag{7}$$

该算法理解为: 随着极化通道间相位中心分离加大, 有效的体散射高度在减少, 结构函数在层的顶部被“压缩”, 变得更加局部化, 体散射去相干也在减少, 这时可用 SINC 函数来弥补由相位信息求算高度中没有考虑的植被顶部高度的“压缩”现象。$\boldsymbol{\varepsilon}$ 在不同的结构下取不同的值。有两种极限情况: 结构函数均匀分布(没有衰减), $\boldsymbol{\varepsilon}$=1/2, 散射中心在植被层的中部, 第一项贡献 $\frac{1}{2}k_zh_{\mathrm{v}}$, 由式(3)知, 第二项贡献 $\frac{1}{2}k_zh_{\mathrm{v}}$; 还有一种情况是衰减趋于无穷大, $\boldsymbol{\varepsilon}$=0, 散射相位中心在树冠的顶部, 第一项贡献了 k_zh_{v}, 第二项为 0。由此可以看出, 该算法能够对这两个极端之间的任意情况做较好的估计, $\boldsymbol{\varepsilon}$ 取值一般为 0.4(Cloude, 2006)。

选择 HV 为体散射占主导的极化通道, 计算 $\gamma_{w_{\mathrm{v}}}$, HH-VV 为表面散射占主导的极化通道, 计算 $\gamma_{w_{\mathrm{s}}}$, 利用(7)式进行反演, 其结果和真实数据的散点图如图 8(a)。该结果的相关性不是很高(表 1)。即使用一个平均非体去相干因子 0.9 来补偿非体去相干的影响(图 8(b)), R^2 仍较低, 说明从物理机制上选择的两个极化通道并没有达到“相位中心不断地分离以达到两相位中心距离最远, 获得纯净的体散射”的目的。

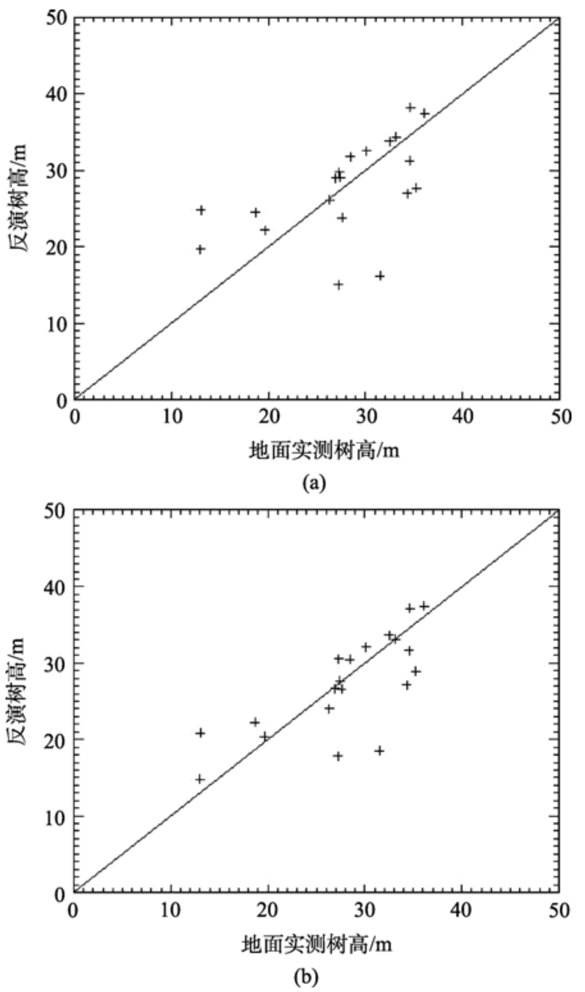

图 8 基于相干相位-幅度综合反演法求算的平均树高和地面实测平均树高的散点图

(a) 未进行非体散射去相干补偿; (b) 进行了非体散射去相干补偿

5 对相干相位-幅度综合反演法的改进

为了达到“相位中心不断地分离以达到两相位中心距离最远, 获得纯净的体散射”的目的, 本文从极化干涉优化的角度出发, 利用可使相位中心最大限度分离的相干优化方法(PD 极化相干优化方法)进行体散射、地表散射极化通道的选择。

这种相干优化方法的基本思想是找到使复相干相位角(式(8))有最大余切的极化组合, 这可以通过解式(9)的特征值问题实现。Ω^{12} 中既含有极化信息, 又有干涉信息, 是式(10)相干矩阵 T 中的元素, 其中 $\boldsymbol{k}=\frac{1}{\sqrt{2}}\begin{bmatrix}S_{\mathrm{HH}}+S_{\mathrm{VV}}\\S_{\mathrm{HH}}-S_{\mathrm{VV}}\\2S_{\mathrm{HV}}\end{bmatrix}$, <>表示多视操作, 脚注 1、2 分别表示在空间基线两端的测量。

$$\cot(\angle\tilde{\gamma})=\frac{\mathrm{Re}\{\tilde{\gamma}\}}{\mathrm{Im}\{\tilde{\gamma}\}}=\frac{\boldsymbol{w}^*(\Omega_{12}+\Omega^*_{12})\boldsymbol{w}}{\boldsymbol{w}^*[-\mathrm{j}(\Omega_{12}-\Omega^*_{12})]\boldsymbol{w}}\tag{8}$$

$(\hat{\Omega}_{12}+\hat{\Omega}^*_{12})\boldsymbol{w}=-\mathrm{j}\lambda(\hat{\Omega}_{12}+\hat{\Omega}^*_{12})\boldsymbol{w}$ 其中

$$\hat{\Omega}_{12}=\hat{\Omega}_{12}\mathrm{e}^{\mathrm{j}(\frac{\pi}{2}-\angle tr(\Omega_{12}))}\tag{9}$$

$$T\leqslant\begin{bmatrix}\boldsymbol{k}_1\\\boldsymbol{k}_2\end{bmatrix}\begin{bmatrix}\boldsymbol{k}_1^{*\mathrm{T}} & \boldsymbol{k}_2^{*\mathrm{T}}\end{bmatrix}\geqslant\begin{bmatrix}[T_{11}] & [\Omega_{12}]\\ [\Omega_{12}]^{*\mathrm{T}} & [T_{22}]\end{bmatrix}\tag{10}$$

式(9)的特征矢量矩阵中, 3×3 矩阵的(0, 0)位置相应于高相位中心极化矢量, (2, 2)位置相应于低相位中心极化矢量。该方法使相位中心得到最大的分离, 高相位就对应到较为“纯净”的体散射相位, 而低相位就对应到较为“纯净”的地表散射相位。

分别用高相位中心极化矢量和低相位中心极化矢量代入式(11),

$$\tilde{\gamma}=\frac{\boldsymbol{w}^{*\mathrm{T}}\Omega_{12}\boldsymbol{w}}{\boldsymbol{w}^{*\mathrm{T}}T\boldsymbol{w}}\ \text{其中}\ T=(T_{11}+T_{22})/2\tag{11}$$

求得式(7)中的 $\tilde{\gamma}_{w_v}$ 和 $\tilde{\gamma}_{w_s}$，进而获得 20 块样地的平均树高，和地面实测平均树高做比较，散点分布图见图 9(a)，仍然有一定程度的高估。用一个平均非体去相干因子 0.9 来补偿非体去相干的影响后的结果如图 9(b)，反演效果得到了进一步改善。

表 1 列出了本文所述各种反演方法的几项定量评价指标。可以看出，DEM 差值算法的 RMSE 最大，R^2 最低，是最差的反演算法。先利用 PD 极化相干优化算法选择体散射、表面散射相干，再进行 DEM 差值反演，使 R^2 提高到 0.503。若将 PD 极化干涉优化结果用到相干相位-幅度综合反演方法中，R^2 从 0.286 提高到 0.678，RMSE 从 6.288m 降低到 5.206m，说明 PD 干涉相干优化对散射相位中心的分离是很有效的。我们通过进一步考虑非体散射去相干的补偿，使 RMSE 减小到 3.343m，是所有方法中最小的，R^2 达到 0.809。

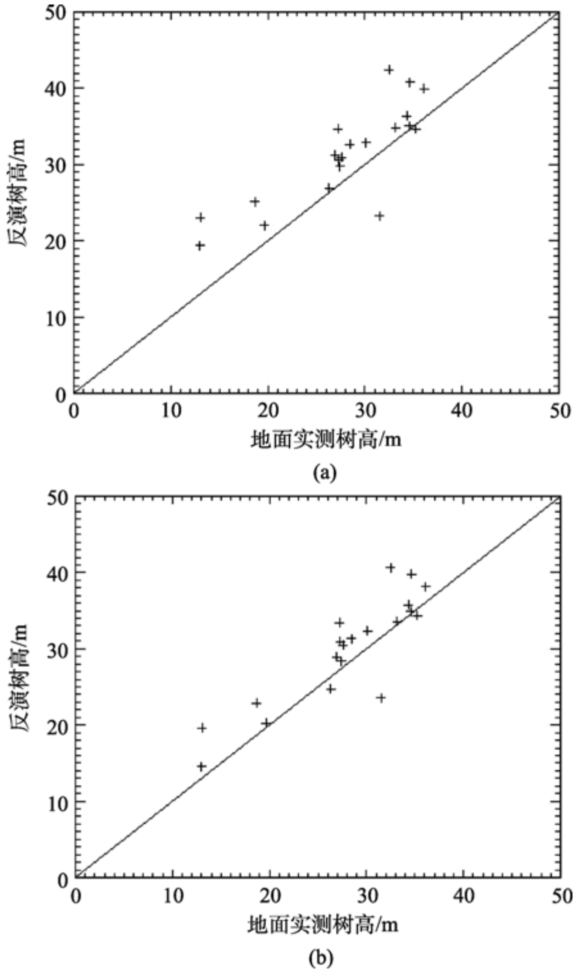

图 9　基于改进的相干相位-幅度法求算的平均树高与地面实测平均树高的散点图

(a) 未进行非体散射去相干补偿；(b) 进行了非体散射去相干补偿

图 10 给出了几种反演算法的剖面图(沿图 1 中的直线)，从图 10 看出，本文发展的改进算法(绿线)对反演结果具有很明显的改善作用。

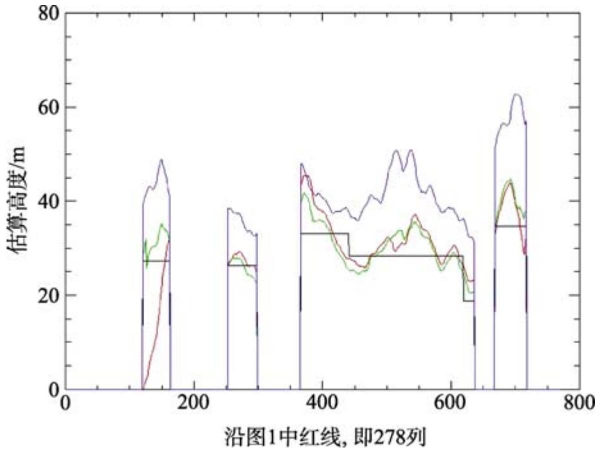

图 10　3 种反演方法估计的平均高的方位向高度剖面图

(紫色：SINC 函数反演法；红色：相干相位-幅度综合反演法；绿色：改进的相干相位-幅度综合反演法；黑色：地面实测平均优势树高)

6　结　论

利用 ESAR L-波段重复轨极化干涉 SAR 数据和地面实测林分高度数据，比较评价了多种极化干涉 SAR 森林高度反演算法。结果发现：(1) 非体散射去相干会引起森林高度的高估现象，对干涉相干进行非体散射去相干的补偿可有效消除高估问题；(2) PD 极化干涉相干优化算法对不同散射机制相位中心的分离是有效的，将其用于 DEM 差值法、相干相位-幅度综合反演法都能有效改善反演效果；(3) 相干相位-幅度综合反演法虽然简单，但综合考虑了相干相位和幅度反演各自的低估、高估问题，在对林地状况具有一定的先验知识条件下，可得到较高的估测精度。本文将 PD 极化干涉相干优化和非体散射去相干补偿运用到该算法中，得到了总体效果最好的反演结果。

REFERENCES

Chen E X, Li Z Y, Pang Y and Tian X. 2007. Polarimetric synthetic aperture radar interferometry based mean tree height extraction technique. *Scientia Silvae Sinicae*, **43**(4): 66—71

Chen E X, Li Z Y, Cloude S R, Papathanassiou K P and Pottier E. 2008. Comparison of methods to derive forest height from polarimetric SAR interferometry. DRAGON-1 Final Symposium, Beijing

Chen X, Zhang H and Wang C. 2008. Vegetation parameter extraction using dual baseline polarimetric SAR interferometry data. *Journal of Electronics & Information Technology*, **30**(12): 2858—2861

Cloude S R and Papathanassiou K P. 1998. Polarimetric SAR interferometry. *IEEE Transactions on Geoscience and Remote Sensing*, **36**(5): 1551—1565

Cloude S R and Papathanassiou K P. 2003. Three-stage inversion process for polarimetric SAR interferometry. *IEEE Proc. Radar Sonar Navig.*, **150**(3): 125—134

Cloude S R. 2006. Polarization coherence tomography. *Radio Science*, **41**(4): RS4017.1—RS4017.27

Hajnsek I, Kugler F, Lee S-K and Papathanassiou K P. 2009. Tropical forest parameter estimation by means of PolInSAR: The INDREX-II campaign. *IEEE Transactions on Geoscience and Remote Sensing*, **47**(2): 481—493

Li X W, Guo H D, Li Z and Wang C L. 2005. Method study of vegetation height estimation using SIR-C dual frequency polarimetric SAR interferometry data. *Chinese High Technology Letters*, **15**(7): 79—84

Mette T, Kugler F, Papathanassiou K P and Hajnsek I. 2006. Forest and the random volume over ground-nature and effect of 3 possible error types. Proceedings of 6th European Conference on Synthetic Aperture Radar (EUSAR 2006). Germany: VDE Verlag GmbH

Mette T. 2007. Forest Biomass Estimation from Polarimetric SAR Interferometry. Munich: Munich University of Technology

Neumann M, Ferro–Famil L and Reigber A. 2009. Improvement of vegetation parameter retrieval from polarimetric sar interferometry using a simple polarimetric scattering model. POLInSAR’2009 Conference

Tabb M, Orrey J, Flynn T and Carande R. 2002. Phase diversity: a decomposition for vegetation parameter estimation using polarimetric SAR interferometry. Proceedings of 4th European Synthetic Aperture Radar Conference (EUSAR 2002). Cologne, Germany

Wu Y R, Hong W and Wang Y P. 2007. The current status and implications of polarimetric SAR interferometry. *Journal of Electronics & Information Technology*, **29**(5): 1258—1262

Yang L, Zhao Y J and Wang Z G. 2007. Polarimetric interferometric SAR data analysis based on TLS-ESPRIT of joint estimation of phase and power. *Acta Geodaetica Et Cartographica Sinica*. **36**(2): 163—168

Zhou G Y, Xiong T, Yang J and Zhang W J. 2008. Forest height inversion based on polarimetric SAR interferometry. 2008 9th International Conference on Signal Processing. USA: IEEE

附中文参考文献

陈尔学，李增元，庞勇，田昕．2007．极化合成孔径雷达干涉测量平均树高提取技术研究．林业科学, **43**(4): 66—71

陈曦，张红，王超．2008．双基线极化干涉合成孔径雷达的植被参数提取．电子与信息学报, **30**(12): 2858—2861

李新武，郭华东，李震，王长林. 2005．用 SIR-C 航天飞机双频极化干涉雷达估计植被高度的方法研究．高技术通讯，**15**(7): 79—84

吴一戎，洪文，王彦平. 2007．极化干涉 SAR 的研究现状与启示．电子与信息学报, **29**(5): 1258—1262

杨磊，赵拥军，王志刚．2007．基于功率和相位联合估计 TLS-ESPRIT 算法的极化干涉 SAR 数据分析．测绘学报，**36**(2): 163—168